ELSEVIER

NeuroImage

www.elsevier.com/locate/ynimg
NeuroImage 31 (2006) 187 – 196

A method to produce evolving functional connectivity maps during the course of an fMRI experiment using wavelet-based time-varying Granger causality

João Ricardo Sato,[a,d,*] Edson Amaro Junior,[b,d] Daniel Yasumasa Takahashi,[b] Marcelo de Maria Felix,[b,d] Michael John Brammer,[c] and Pedro Alberto Morettin[a]

[a]*Institute of Mathematics and Statistics, University of São Paulo, Rua do Matão, 1010, Cidade Universitária, CEP 05508-090, São Paulo, S.P., Brazil*
[b]*Department of Radiology, University of São Paulo, Av. Dr. Enéas de Carvalho Aguiar, 255, 3o. andar, Cerqueira César, São Paulo, SP, CEP 05403-001, São Paulo, S.P., Brazil*
[c]*Brain Image Analysis Unit, Institute of Psychiatry, King's College, London, De Crespigny Park, London SE5 8AF, UK*
[d]*NIF-Neuroimagem Funcional-University of São Paulo, Brazil*

Received 10 August 2005; revised 22 November 2005; accepted 25 November 2005
Available online 23 January 2006

Functional magnetic resonance imaging (fMRI) is widely used to identify neural correlates of cognitive tasks. However, the analysis of functional connectivity is crucial to understanding neural dynamics. Although many studies of cerebral circuitry have revealed adaptative behavior, which can change during the course of the experiment, most of contemporary connectivity studies are based on correlational analysis or structural equations analysis, assuming a time-invariant connectivity structure. In this paper, a novel method of continuous time-varying connectivity analysis is proposed, based on the wavelet expansion of functions and vector autoregressive model (wavelet dynamic vector autoregressive-DVAR). The model also allows identification of the direction of information flow between brain areas, extending the Granger causality concept to locally stationary processes. Simulation results show a good performance of this approach even using short time intervals. The application of this new approach is illustrated with fMRI data from a simple AB motor task experiment.

Keywords: fMRI; Connectivity; Dynamic; Time-varying; Wavelets

Introduction

Functional neuroimaging using the BOLD (Blood Oxygen Level Dependent) effect has received considerable attention in the last decade and has become a powerful tool in cognitive neuroscience. Impressive methodological progress has been made since the first description of the effect (Ogawa et al., 1990) and a large number of statistical methods for data analysis have been proposed, although most of them in somewhat ad hoc fashion. So far, image analysis reports in the literature are mainly dedicated to addressing the detection of brain activation. Such approaches ("brain mapping"), though very useful, are unable to address the more fundamental principles that characterize brain dynamics by probing the connectivity information obtainable from the BOLD signal.

Inferring the dynamics of interaction between different neural structures is a crucial step toward understanding neural organization (Sameshima and Baccala, 1999; Friston, 2002). At conceptual level, there is active interest in the formulation of connectivity analysis. Friston has introduced the concept of dynamic causal models (DCM, Friston, 1995; Friston et al., 2003), based on nonlinear input-state-output systems, and a bilinear approximation to dynamic interactions. However, the DCM results rely on the prior connectivity specifications and also on stationarity conditions. A potentially promising approach to addressing some of these issues is the Granger causality concept (Granger, 1969; Sameshima and Baccala, 1999; Baccala and Sameshima, 2001; Roebroeck et al., 2005) which is borrowed from econometrics and based on the notion of the predictability of one signal by another, subject to the time constraint that the effect cannot precede the cause. It is specially suited to study partially ordered linear dependencies in multivariate contexts without assuming any prior connectivity structure. Recently, significant developments have occurred in the analysis of cerebral connectivity. Buchel and Friston (1997) introduced covariance structural equation modeling in fMRI applications. Subsequently, Goebel et al. (2003) and Roebroeck et al. (2005) have proposed the use of vector autoregressive models and shown their utility in the analysis of fMRI experiments. Nevertheless, Granger causality alone is not sufficient to infer effective causal relations, as it is based only on predictive power. Recent developments in

* Corresponding author. Rua Croata 774, ap22., Vila Ipojuca, São Paulo-S.P., CEP 05056-020, Brazil.
E-mail address: jsato@ime.usp.br (J.R. Sato).
Available online on ScienceDirect (www.sciencedirect.com).

1053-8119/$ - see front matter © 2005 Elsevier Inc. All rights reserved.
doi:10.1016/j.neuroimage.2005.11.039

graphical models have worked towards the identification of effective causal links. Eichler (2005) suggested a graphical representation of multivariate data that allows the inference of effective connectivity, even in the presence of latent variables.

In its original form, Granger causality was defined for linear stationary multichannel signals but, as with most biological signals, there is no unique model for fMRI data and no strong theoretical or experimental basis for the assumptions of stationarity of processes. It is widely recognized that incorrect use of these assumptions can lead to incorrect inferences.

Here, we propose a new method: the wavelet dynamic vector autoregressive (DVAR) process, which can be seen as a generalization of vector autoregressive model (VAR). This approach does not require assumptions about the direction of influence. The DVAR model is a multivariate version of the one proposed by Chang and Morettin (2005) and Dahlhaus et al. (1999). Its novel feature lies in directly modeling time-varying coefficients through wavelet bases with a balance between model complexity and interpretability. Wavelet analysis is an area of intense research in statistical signal analysis because of its wide applicability to model nonstationary signals and its deep relationship to time-frequency representation of a signal. Bullmore et al. (2003, 2004) have demonstrated the value of wavelet analysis applied to the BOLD signal as a means of retaining the colored-noise characteristics of the time series during permutation testing of statistical significance, thus highlighting the use of wavelet techniques in fMRI. Our aim was to combine wavelet analysis and the Granger causality concept given by VAR models to extend the methodology available for the study of brain connectivity. Fitting time-varying coefficients using a wavelet basis allowed us to model nonstationary (locally stationary) and nonlinear (locally linear) multichannel signals using Granger causal (VAR) approaches and make inferences about temporal dynamics of neural interactions. Thus, we can infer the connectivity structure of brain regions in a time-varying way.

In this article, a review of Granger causality theory and connectivity is presented, followed by the methodology underlying the new approach. Simulation results are presented and the usefulness of the method is illustrated in an application involving real fMRI data, in a simple sensorimotor experiment.

Granger causality and dynamic connectivity

Granger causality (Granger, 1969) is a concept that originated in the area of econometrics, focusing on understanding the relationships between two time series. Granger (1969) defined the causality in terms of predictability, based on the fact that the effect cannot come before the cause. Subsequently, Goebel et al. (2003) applied Granger causality to the description of interregional connectivity in fMRI data and to detection of the direction of information flow between brain regions.

Formally, consider a k-dimensional multivariate time series $\mathbf{y}_t$

$$\mathbf{y}_t = [y_{1t}\ y_{2t}, \ldots,\ y_{kt}]',$$

composed by k time series measured on time t. The Granger causality identification is based on the improvement in predictions of future values of the series $\mathbf{y}_t$, using the information of a collection of p past values of the series $(\mathbf{y}_{t-1}, \mathbf{y}_{t-2}, \ldots, \mathbf{y}_{t-p})$. Hence, consider a k-dimensional vector autoregressive model (VAR) of order p, defined by

$$\mathbf{y}_t = \mathbf{v} + \mathbf{A}_1\mathbf{y}_{t-1} + \mathbf{A}_2\mathbf{y}_{t-2} + \ldots + \mathbf{A}_p\mathbf{y}_{t-p} + \boldsymbol{u}_t,$$

where $\boldsymbol{u}_t$ is an error vector of random variables with zero mean and covariance matrix $\boldsymbol{\Sigma}$ given by

$$\sum = \begin{bmatrix} \sigma_{11}^2 & \sigma_{21} & \cdots & \sigma_{k1} \\ \sigma_{12} & \sigma_{22}^2 & \cdots & \sigma_{k2} \\ \sigma_{13} & \sigma_{23} & \cdots & \sigma_{k3} \\ \vdots & \vdots & \ddots & \vdots \\ \sigma_{1k} & \sigma_{2k} & \cdots & \sigma_{kk}^2 \end{bmatrix},$$

and $\mathbf{v}$ and $\mathbf{A}_i$ ($i = 1,2, \ldots, p$) are coefficient matrices given by

$$\mathbf{v} = \begin{bmatrix} v_1 \\ v_2 \\ \vdots \\ v_k \end{bmatrix} \qquad \mathbf{A}_i = \begin{bmatrix} a_{11i} & a_{21i} & \cdots & a_{kl1} \\ a_{12i} & a_{22i} & \cdots & a_{k2i} \\ a_{13i} & a_{23i} & \cdots & a_{k3i} \\ \vdots & \vdots & \ddots & \vdots \\ a_{1ki} & a_{2ki} & \cdots & a_{kki} \end{bmatrix}.$$

The VAR model allows an easy way of identifying Granger causality. An important result of the VAR model, is that the series y_{jt} noncauses y_{lt}, if and only if, the coefficient $a_{jli} = 0$ for any i. In other words, the past values of y_{jt} aid the prediction of future values of y_{lt}. Hence, Granger causalities can be identified simply looking for the VAR representation, and the direction of causality can be interpreted as the direction of information flow. Furthermore, Granger causality relationship is not necessarily reciprocal, for example, y_{jt} may Granger cause the signal y_{lt}, without any implication that y_{lt} Granger causes y_{jt}.

This approach can be extended to the analysis of time series of BOLD signals in functional magnetic resonance imaging data (Goebel et al., 2003). Let k-dimensional time series represent the regions of interest BOLD signal. Using the concept of Granger causality, the VAR modeling makes possible the identification of functional connectivity between brain areas by simply testing the significance of the estimates of the components of the matrix $\mathbf{A}_t$. However, as the Granger causality is defined in terms of predictability, the VAR modeling can indicate only functional relationships. In other words, this approach points out the links between signals, but does not, per se, indicate neurophysiologic mechanisms (effective connectivity).

There are two widely used approaches to assigning significance to the elements of matrices $\mathbf{A}_i$. The first is based on a Wald test for the statistical significance of the causality coefficients of a VAR model (Lütkepohl, 1993). The second one is based on the computation of F statistics by considering the ratio of residual variances and is described in detail by Geweke (1982).

According to Roebroeck et al. (2005), there are two main obstacles to the application of Granger causality mapping in fMRI. The first obstacle is that the BOLD response is not a direct measure of neural activity, and then, the connectivity relationships cannot be identified due to hemodynamic blurring. Furthermore, the low temporal resolution of fMRI may not provide enough information for inferring connectivity. Despite these apparent problems, the above authors were able to show by simulations that the Granger causality can be useful for inferring brain functional connectivity.

However, VAR modeling is an adequate approach only in cases of stationary time series, i.e., the autoregressive coefficients and error matrix covariance are time-invariant. In fact, most connectivity studies of fMRI data to date have used correlation analysis or structural equations models, assuming stationarity conditions. In

order to overcome this limitation, we propose a new approach using dynamic VAR (DVAR), defined by

$$\mathbf{y}_t = \mathbf{v}(t) + \mathbf{A}_1(t)\mathbf{y}_{t-1} + \mathbf{A}_2(t)\mathbf{y}_{t-2} + \ldots + \mathbf{A}_p(t)\mathbf{y}_{t-p} + \boldsymbol{u}_t,$$

where $\boldsymbol{u}_t$ is an error vector of random variables with zero mean and covariance matrix $\boldsymbol{\Sigma}(t)$ given by

$$\sum(t) = \begin{bmatrix} \sigma_{11}^2(t) & \sigma_{21}(t) & \cdots & \sigma_{k1}(t) \\ \sigma_{12}(t) & \sigma_{22}^2(t) & \cdots & \sigma_{k2}(t) \\ \sigma_{13}(t) & \sigma_{23}(t) & \cdots & \sigma_{k3}(t) \\ \vdots & \vdots & \ddots & \vdots \\ \sigma_{1k}(t) & \sigma_{2k}(t) & \cdots & \sigma_{kk}^2(t) \end{bmatrix},$$

and $\mathbf{v}(t)$ and $\mathbf{A}_i(t)$ ($i = 1,2, \ldots, p$) are coefficient matrices given by

$$\mathbf{v}(t) = \begin{bmatrix} v_1(t) \\ v_2(t) \\ \vdots \\ v_k(t) \end{bmatrix} \qquad \mathbf{A}_i(t) = \begin{bmatrix} a_{11i}(t) & a_{21i}(t) & \cdots & a_{kl1}(t) \\ a_{12i}(t) & a_{22i}(t) & \cdots & a_{k2i}(t) \\ a_{13i}(t) & a_{23i}(t) & \cdots & a_{k3i}(t) \\ \vdots & \vdots & \ddots & \vdots \\ a_{1ki}(t) & a_{2ki}(t) & \cdots & a_{kki}(t) \end{bmatrix}.$$

In other words, in this case, we allow a time-variant structure for the intercept, autoregression coefficients and covariance matrix. Time-varying autoregressive models have previously been estimated using adaptative filters or windowed models. However, these approaches are suitable only in the context of time-series with many sample points. Many (probably most) fMRI data do not satisfy this criterion. Furthermore, the classical windowed models do not allow efficient estimation in cases of replications of conditions, as the AB periodic experiments. Here, a wavelet-based dynamic multivariate autoregression estimation is proposed, and its usefulness illustrated by simulations and an application to a real fMRI experiment.

A wavelet approach

Firstly, let an orthonormal basis generated by a mother wavelet function $\psi(t)$,

$$\psi_{j,k}(t) = 2^{j/2}\psi\left(2^j t - k\right), \quad j,k \in Z,$$

and assume the following properties:

(i) $\int_{-\infty}^{\infty} \psi(t)\mathrm{d}t = 0$

(ii) $\int_{-\infty}^{\infty} |\psi(t)|\mathrm{d}t < \infty$

(iii) $\int_{-\infty}^{\infty} \frac{|\Psi(\omega)|^2 \mathrm{d}\omega}{|\omega|} < \infty$, where the function $\psi(\omega)$ is the Fourier transform of $\psi(t)$.

(iv) $\int_{-\infty}^{\infty} t^j \psi(t)\mathrm{d}t = 0$, $j = 0,1, \ldots, r-1$ for $r \geq 1$ and $\int_{-\infty}^{\infty} t^j \psi(t)\mathrm{d}t = 0$.

An important result is that any function $f(t)$ with $\int_{-\infty}^{\infty} f^2(t)\mathrm{d}t < \infty$ can be expanded as

$$f(t) = \sum_{j=-\infty}^{\infty} \sum_{k=-\infty}^{\infty} c_{j,k}\psi_{j,k}(t).$$

In other words, the function $f(t)$ can be represented by a linear combination of functions $\psi_{j,k}(t)$. Therefore, considering the time-varying VAR model, the autoregressive coefficient functions $a_{lmi}(t)$ can be expanded as

$$a_{lmi}(t) = \sum_{j=-\infty}^{\infty} \sum_{k=-\infty}^{\infty} c_{j,k}^{(i)}\psi_{j,k}(t).$$

In practice, we use a truncated wavelet expansion, given by

$$a_{lmi}(t) = c_{-1,0}^{(i)}\phi(t) + \sum_{j=0}^{J} \sum_{k=0}^{2^j-1} c_{j,k}^{(i)}\psi_{j,k}(t).$$

where the time series extension T is a power of two, $\phi(t)$ is called the scale function and $c_{j,k}(i)$ ($j = -1,0,1, \ldots T-1$; $k = 0,1,2, \ldots, 2^j - 1$; $i = 1,2, \ldots p$) are the wavelet coefficients for the i-th autoregressive coefficient function $a_{lmi}(t)$. As the basis functions $\phi(t)$ and $\psi_{jk}(t)$ are known, the task of estimating the dynamic autoregressive parameters consists of the estimation of each of the wavelet coefficients $c_{j,k}^{(i)}$ for all the autoregressive functions in the matrices $\mathbf{A}_i(t)$ ($i = 1,2, \ldots, p$), the intercept functions in $\mathbf{v}(t)$ and the covariance functions in $\boldsymbol{\Sigma}(t)$.

A very important point is the choice of the maximum resolution scale parameter J. This task is strongly related to previous information about the smoothness of the curve to be estimated. If we desire to capture more details or a high level of adaptability, a large value of J has to be chosen. However, there is a trade off to be considered, as large values of J imply large variances. Hence, we concluded that the maximum scale parameter has to be chosen according to the expected degree of smoothness of the connectivity changes.

Maximum likelihood estimation is not efficient in this case, due to the large number of parameters to be estimated. Dahlhaus et al. (1999) suggested an estimation approach in the univariate case, and we have generalized it to multivariate time series. We propose the use of an interactive generalized least square estimation procedure, which is composed by a loop of two stages. In the first stage, the parameters of $\mathbf{A}_i(t)$ and $\mathbf{v}(t)$ are estimated using a generalized least squares estimation. Then, in the second stage, the covariance functions in $\boldsymbol{\Sigma}(t)$ are estimated using the residuals of the first stage. These two steps are repeated until the convergence of the parameters, or until a certain number of maximum interactions is achieved, as an extension of the Cochrane and Orcutt procedure. Details of the estimation procedure and asymptotical statistical results are presented in Appendix A. Statistical tests of the significance of the coefficients and connectivities were undertaken using Wald tests, and details are also included in Appendix A. In this work, we chose the extreme phase daublets 8 wavelet basis proposed by Daubechies (1988), with periodic boundary conditions, but the results are applicable to any wavelet basis. Optimal use of wavelets optimal requires a power of 2 time series length.

Simulations

In order to evaluate the DVAR approach to fMRI connectivity analysis, we simulated 1000 five-dimensional dynamic autoregressive models of order 1. We consider an AB periodic structure with six cycles of length 16, assuming that each cycle has the same time-

varying connectivity structure. Hence, supposing the five series are BOLD signals of five different brain areas, we evaluated the performance and usefulness of the novel method. The model and theoretical functions of these simulations are described in Appendix A. The DVAR model estimation procedure was applied to the signals in each simulation and the results are shown in Fig. 1.

The simulations show that the average of each of the estimated curves is close to the theoretical ones. Further, the estimates do not have a high variability, indicating that the DVAR approach has good performance. Consider the connectivity function map shown in Fig. 1 as an illustrative example of a model to be interpreted. The panel (3->4) indicates the flow of information from the third series to the fourth, and the flow is higher in the middle of the cycle. The absolute values of the connectivity function measure the degree of the flow of information. If the connectivity function is negative, it can be interpreted as a negative impact, i.e., an increase in the sender's signal is followed by a decrease in the receiver's signal.

A very important point to be highlighted in these simulations is the nonprespecification of connectivity structure. All possible connections are considered without any inclusion of exogenous variables or subjective assumptions. Thus, if two areas are disconnected during all the cycle, the connectivity function is zero for each time point as shown in panel (2->5). Statistical tests about the parameters of the model can also be tested using a Wald contrast test, which is described in Appendix A. Hence, connectivity tests in any time interval can be performed. We say that an area A is sending information to another area B, if and only if the connectivity function from A to B is nonzero. Thus, the Wald test can be very useful to inferring the connectivity structure at any time point, as the estimated connectivity functions are linear combinations of the parameters (contrasts).

Application to fMRI real data

The DVAR approach was applied to two subjects who performed motor tasks in a simple AB block design. The images were acquired in a GE 1.5 T Signa MR system equipped with a 23 mT/m gradient (TE 40 ms, TR 3000 ms, FA 75°, FOV 240 mm, 64 × 64 matrix; 8 slices, thickness 7.0 mm, gap 0.7 mm) oriented in the AC–PC plane in a single run. Sixty volumes were acquired during three cycles of rest-task performance (each one with 60 s and 20 images) and the total imaging time for each run was 3:12 min (which included 4 TR to achieve steady-state transverse magnetization). Both subjects were normal, right-handed females. During the MR imaging, the subjects lay in the dark with a noise-reducing headphones that were customized for functional MR imaging experiments and provide isolation from scanner noise. The AB block design experiment paradigm consisted of alternating (condition A) rest and (condition B) right hand self-paced finger tapping movements.

The volumes were motion corrected and spatially smoothed (Brammer et al., 1997). The responses at each voxel were modeled by Poisson functions and activation maps were obtained using a nonparametric approach (Brammer et al., 1997; Brammer, 1998; Bullmore et al., 1999, 2001, 2003; Breakspear et al., 2004). The areas detected as active (cluster P value = 0.01) are shown in Fig. 2.

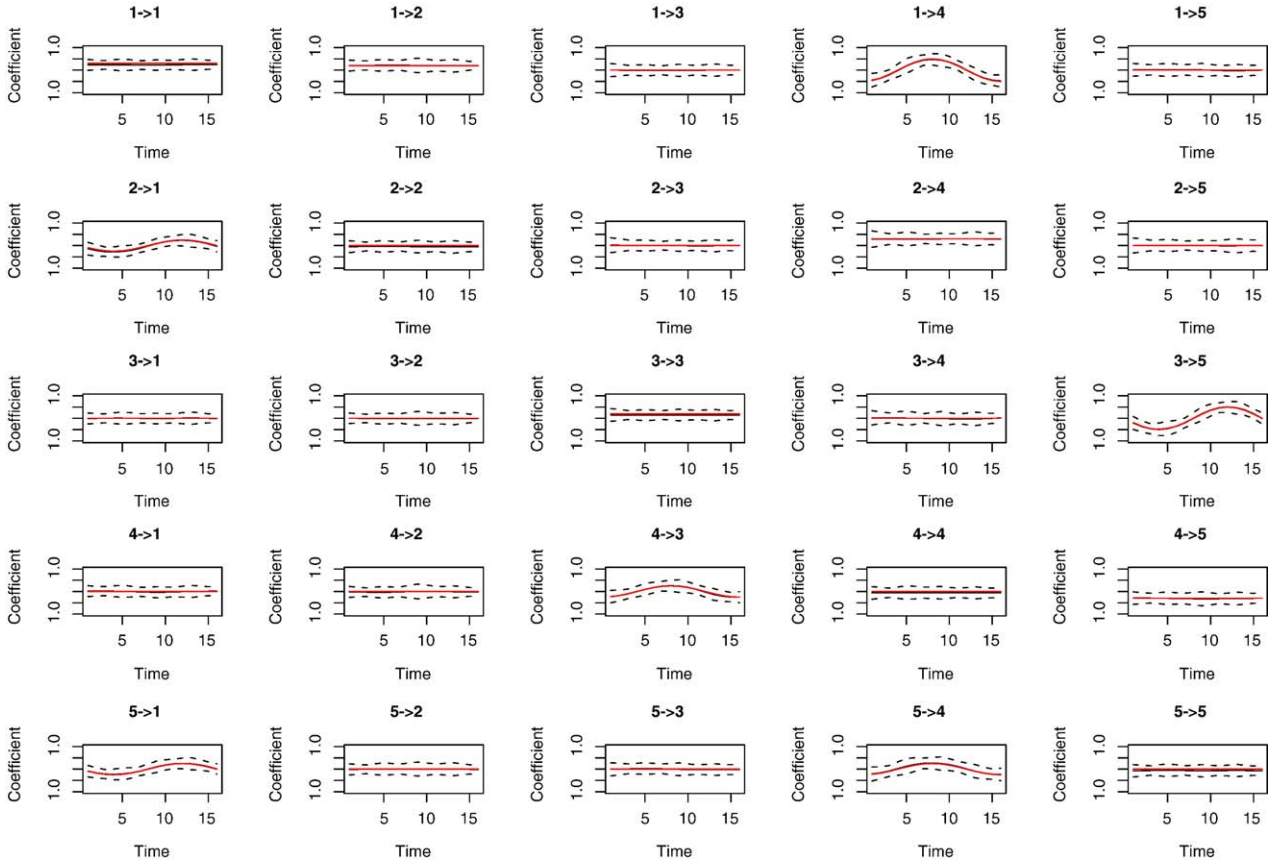

Fig. 1. Simulation results of five-dimensional time series. The solid red line is the theoretical connectivity function $\mathbf{A}_1(t)$ and the solid black line is the average of the estimated curves. The ticked lines are the band of one standard error.

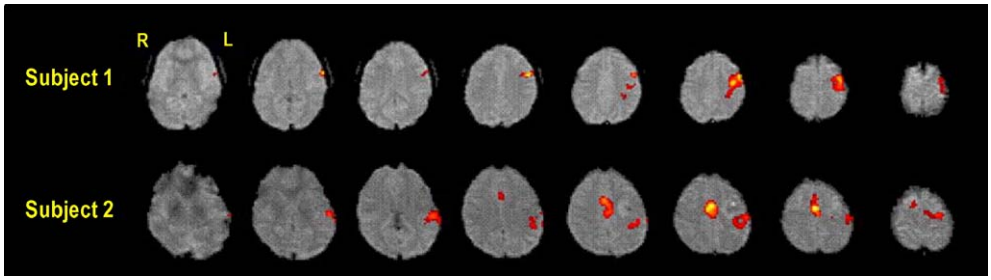

Fig. 2. Activated areas detected during the finger tapping of two subjects in a motor experiment (radiological notation).

The first illustration of the use of DVAR to real fMRI data involved a multiple bivariate approach. In this analysis, we selected one ROI of 5 × 5 voxels centered in the local maximum of the primary motor area (M1) in one slice. The three AB cycles originally composed by 20 volumes were reduced to 16 volumes by cubic splines interpolation, allowing the use of Daubechies periodic double extreme phase wavelets. The wavelet DVAR approach of order 1 was applied to bivariate models using this ROI average signal and each remaining intracerebral voxel. This is a time-varying extension of the approach used by Goebel et al. (2003). The connectivity maps (Figs. 3 and 4) were smoothed using a Gaussian kernel filter (FWHM 5 mm). The maps show the temporal information flow intensity changes (from each voxel to the ROI) during the AB cycle, measured by the connectivity functions (with threshold in absolute values less than 0.9). The maps can also be thresholded by computing the value of the estimated connectivity for significance at a particular chosen P value, using the Wald test (in Appendix A).

The images show a pattern of bivariate relationships with signal variation in prefrontal regions initially explaining the M1 time-series variability. This relationship (in the rest phase) evolves to include parietal areas and premotor regions. This slice also shows that signal changes in M1 are also highly predicted by its own previous behavior during both rest and active epochs.

In the second subject, we have also found that areas with signal variations explaining the signal change in M1 occur in the prefrontal cortex during the rest epoch, and proceed to a more parietal and premotor distribution during the active phase. Likewise, the M1 signal change is also predicted by its own history of signal changes, and in this case markedly during the moments where the subject was finger tapping with the contra lateral hand.

The DVAR model can also be applied to preselected ROIs, in a k-dimensional modeling. We preselected five ROIs from the connectivity maps of subject two, including the local maxima of the left primary motor cortex in the precentral gyrus (LM1), left Anterior Cingulate gyrus (ACg), a medial superior medial frontal gyrus, centered on the Supplementary motor area (SMA), right anterior back of the precentral gyrus, the right premotor cortex (RpM1) and superior dorsal aspect of the medial parietal lobe, the anterior precuneus (ApC). These areas are implied in movement control (Kermadi et al., 2000; Wenderoth et al., 2005a,b) and are shown to participate in motor learning skills (Jancke et al., 2000; Kurata et al., 2000). The DVAR model was applied to the data and a Wald test for

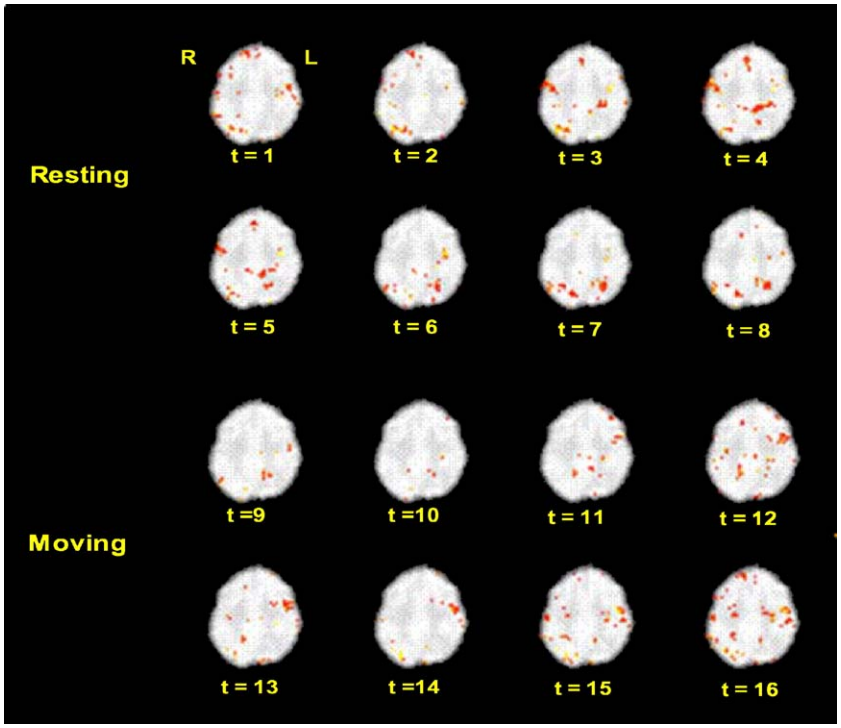

Fig. 3. Subject one connectivity map. The map shows the voxel to ROI information flow intensity, estimated by connectivity functions of the DVAR model.

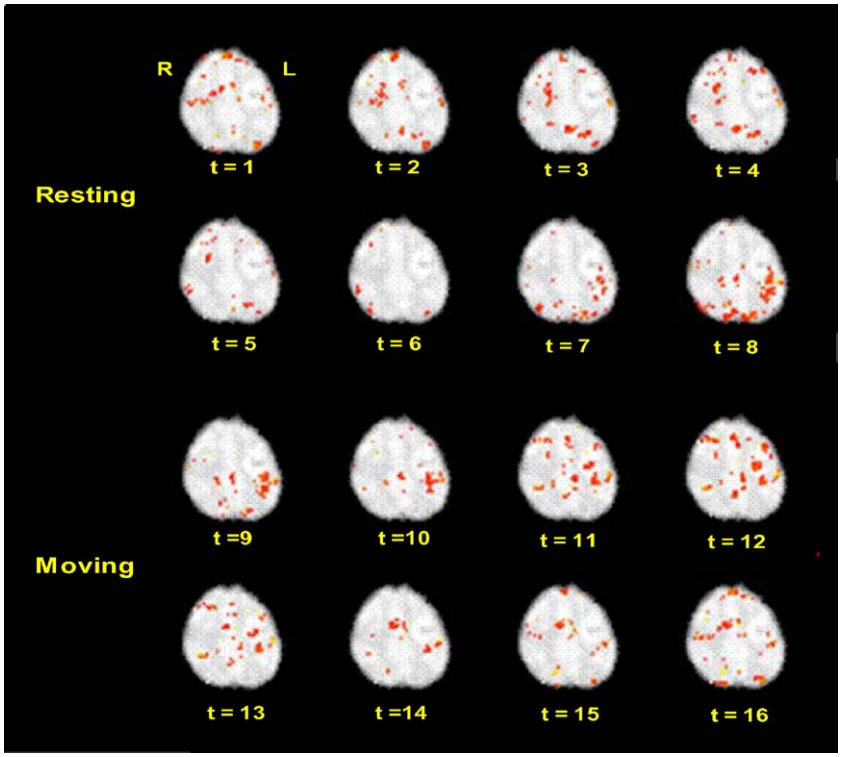

Fig. 4. Subject two connectivity map. The map shows the voxel to ROI information flow intensity, estimated by the connectivity functions.

significant connectivities (see Appendix A) was carried out. The ROI connectivity diagram showing the significant links (P value < 0.05) is depicted in Fig. 5.

The analysis of the temporal evolution of the connectivity between the areas shows an influence of the SMA and ApC in the LM1 during the rest period, which is reduced during the movement epoch, with a subtle inversion of this influence at the first two images of this period. Conversely, the flow of information from the LM1 to the RpM1 displays a reversed pattern, with most of the BOLD effect predicted (and in opposite signal) in the RpM1 during the rest period changing to a positive influence during the movement period. The relation between ACg and SMA is somewhat more complex, with an enhanced positive connectivity in the transitions between rest and movement, and a negative connectivity in the rest period, which is even more evident in the movement period.

Discussion

The main advantage of the wavelet-based dynamic autoregressive model (DVAR), compared with other connectivity models is that it avoids stationarity and linearity assumptions. It is well known that different tasks involve different circuitries, and is widely believed that the brain exhibits dynamic alterations in interregional connectivity. Hence, the adoption of probably unwarranted stationarity assumptions may lead to spurious results. Furthermore, the DVAR approach does not require model prespecification, unlike structural equation modeling (Buchel and Friston, 1997), and this may be desirable as in the illustrations above. ROI preselections or prespecification represent particular cases of the DVAR model.

Classical dynamic models are based on local fitting using a moving window. However, the detection of dynamic changes by this approach may have poorer time-resolution and be less flexible than that achieved by wavelet-based methods (Dahlhaus et al., 1999). Further, replications of conditions as an AB experiments can be easily modeled by periodic wavelets.

The engagement of prefrontal regions observed in our data as the source of information to the primary motor region is expected during the initial moments of the active epoch, and is consistent with previous studies of motor preparation (Lee et al., 1999; Ohara et al., 2001; Cunnington et al., 2002). The detection of premotor and supplementary areas as 'predictors' of the BOLD signal change of the primary motor region is also expected, since the involvement of those regions has already been demonstrated in previous studies relating to motor preparation (Cui et al., 2000; D'Esposito et al., 2000; Toni et al., 2001). On the other hand, these regions are constantly sending information to the primary motor cortex across the experiment, which may thus represent a monitoring process, and perhaps could be modulated by habituation, or training, processes. In fact, the left premotor region is evident in the connectivity map only in the active epochs, and is not involved in sending information to the primary motor region in the rest epoch in subject 2.

In addition, towards the end of the "rest" epoch, we detected an increased participation of the parietal regions, possibly related to monitoring of movements (Coull et al., 2000; Hall et al., 2000; Lutz et al., 2000). The prefrontal regions are possibly modulating the information flow to the primary motor region the rest period, especially at the beginning of the epoch. This could be due to an inhibitory process and attentional load, as this area has been described as a putative center for top-down control of the information in the network.

When analyzing the connectivity map from the five predefined regions, the pattern of connectivity is even more interesting, since we have more precise information regarding the sign of the

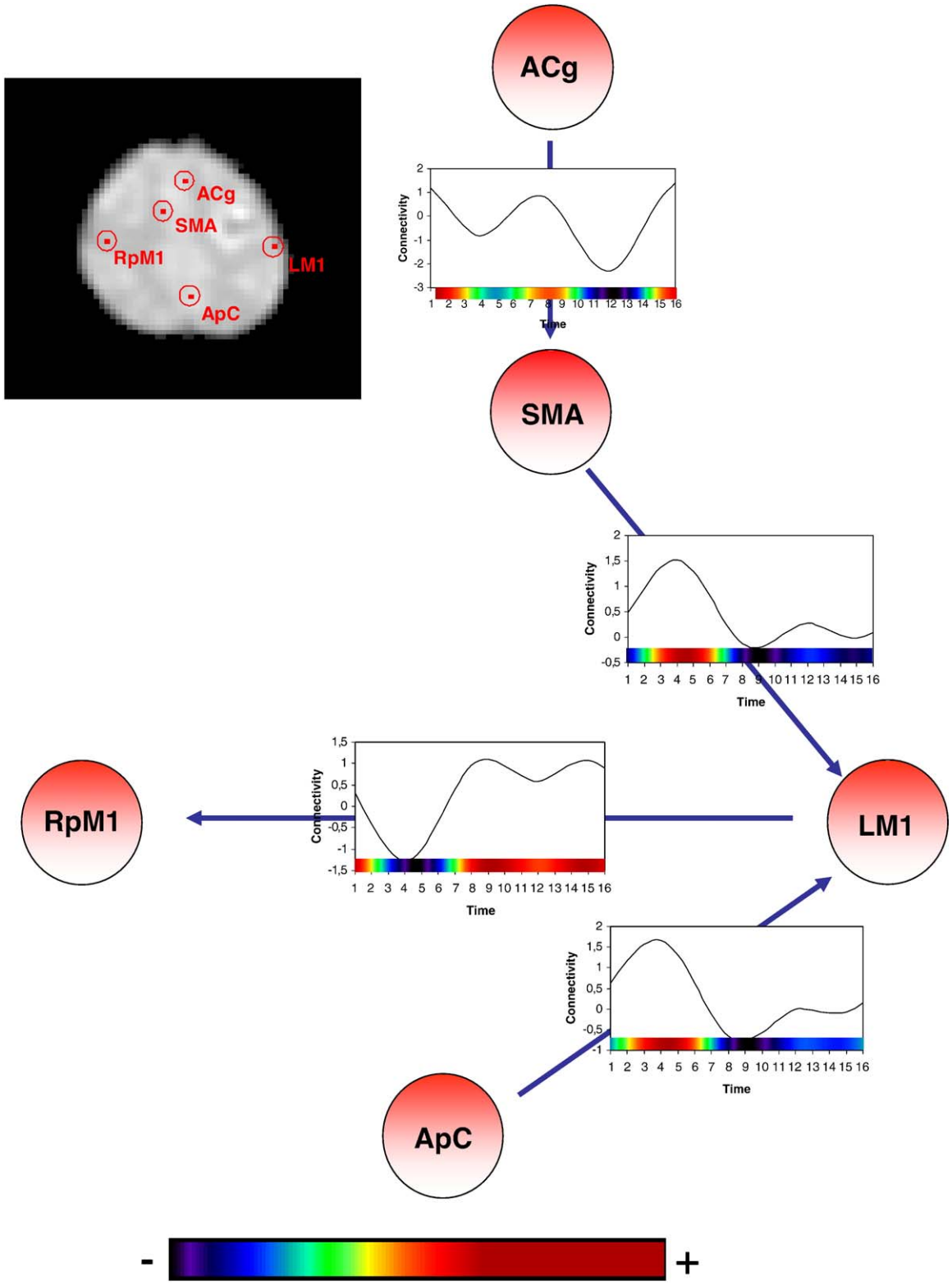

Fig. 5. Significant ROI connectivities. The connectivity functions are shown in each arrow.

connectivity. It is expected that the BOLD effect in areas hierarchically organized in movement control can be used to infer modulation, or influence, in the BOLD effect in the primary motor area. The pattern of temporal evolution found in the connectivity map is clearly very informative in at least one sense: the information flow is in agreement to what one can predict from previous studies in humans and animal models (Stephan et al., 1999; Kermadi et al., 2000), though further work is needed. The ACg is believed to mediate the processes involved in integration and bimanual control, and as well as SMA is involved in both complexity and frequency of

hand movement (Debaere et al., 2004; Wenderoth et al., 2004, 2005a,b). The dorsal anterior precuneus region is believed to be involved in the attentional aspect of the motor task (Wenderoth et al., 2005a,b). In our analysis, the temporal evolution of the connectivity between this area and the primary motor region suggests that most of its influence is observed in the rest period, perhaps reflecting expectation. One may expect this pattern to change during bimanual tasks (Wenderoth et al., 2005a,b). The fact we are detecting this area as modulating activity in the primary motor area in the rest is in agreement with the concept of its participation in a "default mode network" (Raichle et al., 2001).

Another interesting pattern of connectivity emerging from this preliminary analysis is the supra-periodicity variation of the flow of information between the ACg and SMA. The participation of these areas during the planning of the movement, but not execution of bimanual movements was described by Viallet et al. (1992). Furthermore, SMA region is not unique, and pre-SMA neurons are more active during movement preparation than execution (Matelli et al., 1991; Luppino et al., 1993; Rizzolatti et al., 1996). In our analysis, the flow of information between ACg and SMA is 'switched on' during the transitions between conditions, and decays during the middle of the epochs congruent with the idea of participation of these areas in selection of action sets (Rushworth et al., 2004). This type of information could be used to check the assumption that ACg has a modulatory influence in SMA activity in bimanual tasks, as was predicted by the literature (Boecker et al., 1998; Wenderoth et al., 2005a,b).

Clearly, these are preliminary data, but nonetheless they are in reasonable agreement with current opinion in motor planning and execution. We have also used only the original epi images as the source of time-series, instead of using time-series from images previously transformed to a common space. The reason for our choice was to avoid the interference from automatic spatial transformation algorithms, and was based on a high variability of the medial frontal functional regions among subjects (Stephan et al., 1999). Even so, caution should be taken when interpreting the connectivity maps regarding anatomical location of the areas in the model. Although the distinction between SMA and ACg is not defined, even cytoarchitectonic, we used the definition from Stephan et al. (1999) as these authors have described the structures in individual subjects based on anatomical landmarks. Nevertheless, our method does not depend on the adopted procedure for neuroanatomical region selection, and could be used with template brains and Talairach coordinates if the user wishes to (Talairach and Tournoux, 1988).

Although these are preliminary observations, it is evident that the method can produce valuable information about brain function as probed by BOLD images. We believe that this analysis may provide useful insights into the investigation of neural networks using fMRI, free from some of the limitations implicit in much existing methodology.

Conclusion

Understanding neural connectivity is widely recognized as being essential for the understanding of brain function. Nevertheless, the complexity and time-varying properties of cerebral signals sampled by techniques such as fMRI are obstacles for the application of classical stationary models, because different tasks or states demand different brain circuitries and directions of information flow across time. Instead of providing only one connectivity structure for the entire experiment, our technique provides different structures for each time point. We propose a wavelet-based time-varying connectivity analysis trying to overcome the constraints of stationary models, and illustrated its usefulness with plausible results using real fMRI data sets.

Acknowledgments

We like to thank the reviewers for the insightful and useful suggestions and the financial support provided by CAPES, CNPq(142616/2005-2) and FAPESP(03/10105-2)/Brazil.

Appendix A. Estimation algorithm and statistical properties

In this section, the estimation procedure and some useful statistical results are presented. Let $\mathbf{y}_t$, a k-dimensional multivariate time series with length T, modeled by a time-varying VAR process of order p. Consider the following matrices

$$\mathbf{Y}_{t-l} = \begin{bmatrix} y_{1,(p-l+1)} & y_{2,(p-l+1)} & \cdots & y_{k,(p-l+1)} \\ y_{1,(p-l+2)} & y_{2,(p-l+2)} & \cdots & y_{k,(p-l+2)} \\ \vdots & \vdots & \ddots & \vdots \\ y_{1,(T-l)} & y_{2,(T-l)} & \cdots & y_{k,(T-l)} \end{bmatrix},$$

$$\mathbf{U} = \begin{bmatrix} u_{1,(p+1)} & u_{2,(p+1)} & \cdots & u_{k,(p+1)} \\ u_{1,(p+2)} & u_{2,(p+2)} & \cdots & u_{k,(p+2)} \\ \vdots & \vdots & \ddots & \vdots \\ u_{1,T} & u_{2,(T)} & \cdots & u_{k,(T)} \end{bmatrix}$$

and

$$\prod = \begin{bmatrix} \psi_{-1,0}(p+1) & \psi_{0,0}(p+1) & \cdots & \psi_{J,2^J-1}(p+1) \\ \psi_{-1,0}(p+2) & \psi_{0,0}(p+2) & \cdots & \psi_{J,2^J-1}(p+2) \\ \vdots & \vdots & \ddots & \vdots \\ \psi_{-1,0}(T) & \psi_{0,0}(T) & \cdots & \psi_{J,2^J-1}(T) \end{bmatrix}.$$

Let also the row-Kronecker product defined by

$$\begin{bmatrix} a_1 \\ a_2 \\ \vdots \\ a_n \end{bmatrix} \otimes^L \begin{bmatrix} b_1 \\ b_2 \\ \vdots \\ b_n \end{bmatrix} = \begin{bmatrix} a_1 \otimes b_1 \\ a_2 \otimes b_2 \\ \vdots \\ a_n \otimes b_n \end{bmatrix},$$

and the following matrices

$$\mathbf{W} = \left[1_{T-P} \otimes^L \prod \mathbf{Y}_{t-1} \otimes^L \prod \cdots \mathbf{Y}_{t-l} \otimes^L \prod\right],$$

$$\mathbf{M} = \mathbf{I}_k \otimes \mathbf{W},$$

where 1_{T-p} is a column vector of $(T-p)$ ones and $\mathbf{I}_k$ is identity matrix of order k.

Considering that the wavelet expansion of an information flow function from the series y_{lt} to y_{mt} is given by

$$a_{lmi}(t) = \sum_{j=-\infty}^{\infty} \sum_{k=-\infty}^{\infty} c_{j,k}^{(i)} \psi_{j,k}(t),$$
$$\left(j = -1,0,1,\ldots T-1;\ k = 0,1,2,\ldots,2^j-1;\ i = 1,2,\ldots,p\right),$$

and hence, assuming that the random errors covariance matrix $\mathbf{\Sigma}(t)$ for all t is known and considering the vector

$$Z = \mathrm{vec}(\mathbf{Y}_t),$$

the DVAR model can be written as

$$Z = \mathbf{M}\boldsymbol{\beta} + \varepsilon.$$

The parameter $\boldsymbol{\beta}$ is a vector containing all the wavelet expansion coefficients $c_{j,k}^{(i)}$ for all the connectivity functions to be estimated. The error term $\varepsilon = \mathrm{vec}(\mathbf{U})$ is a vector containing all the random errors of all the k series. The covariance matrix of ε is denoted by $\mathbf{\Gamma}$, contains all covariance the matrices $\mathbf{\Sigma}(t)$ ($t = p, p+1, \ldots, T$) and is time-invariant.

Hence, from Graybill (1976), the generalized least square estimator for the parameters of the model is given by

$$\hat{\boldsymbol{\beta}} = \left(\mathbf{M}'\mathbf{\Gamma}^{-1}\mathbf{M}\right)^{-1}\mathbf{M}'\mathbf{\Gamma}^{-1}Z.$$

In practice, the error covariance matrix is unknown and it has to be estimated. A consistent estimator for the time-varying variance for each time series can be obtained considering a wavelet smoothing of the squared residuals (r_{it}^2, $i = 1, \ldots, k$). Furthermore, the time-varying covariances can also be obtained by a wavelet smoothing of the cross-residuals ($r_{it}r_{jt}$, $i = 1, \ldots, k$, $j = 1, \ldots, k$, $i \neq j$).

Hence, we propose an interactive algorithm given by:

(1) Assume $\mathbf{\Gamma} = \mathbf{I}$, and perform the generalized least square estimation;
(2) Compute the residuals and obtain an estimate of the errors time-varying covariance matrix;
(3) Perform the generalized least square estimation considering the estimated covariance matrix;
(4) Go to step 2 and repeat until the convergence of the parameters.

Considering the estimation procedure described, it can be shown (see Hajek-Sidak's Central Limit Theorem, Sen and Singer, 1980) that the asymptotic distribution of the interactive generalized least square estimator is given by

$$\sqrt{kT}\hat{\beta} \sim N(\beta, \mathbf{\Gamma}).$$

Furthermore, the statistical test to the null hypothesis of

$$\mathbf{C}\boldsymbol{\beta} = m,$$

against the hypothesis of inequality can be tested using the Wald Statistic for contrasts given by

$$W = \frac{\left(\mathbf{C}\hat{\boldsymbol{\beta}} - m\right)'\left[\mathbf{M}'\mathbf{\Gamma}^{-1}\mathbf{M}\right]^{-1}\left(\mathbf{C}\hat{\boldsymbol{\beta}} - m\right)}{\mathrm{rank}(\mathbf{C})},$$

where $\mathbf{C}$ is the contrast matrix.

Hence, we can test many hypothesis of connectivity significance or time-varying connectivity performing a Wald test, considering an adequate contrast matrix $\mathbf{C}$. More details about the Wald test for contrasts can be found in Graybill (1976). Any statistical test for the connectivity functions can be performed using the Wald test, as the functions are estimated by linear combinations of the coefficients. For example, the statistical test for a link between two regions can be performed considering the hypothesis that all wavelets expansion coefficients for this connectivity function are zero.

In addition, we can also obtain confidence intervals for the connectivity functions. Let $\hat{\boldsymbol{\xi}}$ a vector containing all estimated coefficients for a wavelet expansion of a function $f(t)$, $\boldsymbol{\delta}(t)$ a vector of the respective wavelets functions in time t and $\mathbf{\Lambda}$ the covariance matrix of $\hat{\boldsymbol{\xi}}$. A natural estimator of $f(t)$ is given by

$$\hat{f}(t) = \hat{\boldsymbol{\xi}}'\boldsymbol{\delta}(t)$$

It can be shown, using Hajek-Sidak's Central Limit Theorem (Sen and Singer, 1980) that asymptotically

$$\hat{f}(t) \sim N(f, \boldsymbol{\delta}\mathbf{\Lambda}\boldsymbol{\delta}'),$$

and hence, confidence intervals for each connectivity function can be obtained using this result.

Simulations

In the Simulations section, we consider a DVAR model of order one, considering the following connectivity matrix

$$\mathbf{A}(t) = \begin{bmatrix} 0 & 0.2 & 0 & \cos\left(\frac{2\pi t}{16} + \pi\right)/2 & 0 \\ \sin\left(\frac{2\pi t}{16} + \pi\right)/4 & 0 & 0 & 0.3 & 0 \\ 0 & 0 & 0.2 & 0 & \sin\left(\frac{2\pi t}{16} + \pi\right)/2 \\ 0 & 0 & \cos\left(\frac{2\pi t}{16} + \pi\right)/4 & 0 & 0.3 \\ \sin\left(\frac{2\pi t}{16} + \pi\right)/4 & 0 & 0 & \cos\left(\frac{2\pi t}{16} + \pi\right)/4 & 0 \end{bmatrix},$$

intercept vector given by

$$\mathbf{v}(t) = \begin{bmatrix} \sin\left(\frac{2\pi t}{16} + \pi\right)/2 \\ 0 \\ \cos\left(\frac{2\pi t}{16} + \pi\right)/4 \\ 0 \\ 0 \end{bmatrix},$$

and error covariance matrix

$$\sum(t) = \begin{bmatrix} 0.49 & 0.147\left(1 + \cos\left(\frac{2\pi t}{16}\right)/6\right) & 0 & 0 & 0 \\ 0.147\left(1 + \cos\left(\frac{2\pi t}{16}\right)/6\right) & 0.53\left(1 + \cos\left(\frac{2\pi t}{16}\right)/6\right) & 0 & 0 & 0 \\ 0 & 0 & 0.49 & 0 & 0 \\ 0 & 0 & 0 & 0.49 & 0.0.147 \\ 0 & 0 & 0 & 0.147 & 0.0341 \end{bmatrix}.$$

References

Baccala, L.A., Sameshima, K., 2001. Partial directed coherence: a new concept in neural structure determination. Biol. Cybern. 84 (6), 463–474.

Boecker, H., Dagher, A., et al., 1998. Role of the human rostral supplementary motor area and the basal ganglia in motor sequence control: investigations with H2 15O PET. J. Neurophysiol. 79 (2), 1070–1080.

Brammer, M.J., 1998. Multidimensional wavelet analysis of functional magnetic resonance images. Hum. Brain Mapp. 6 (5–6), 378–382.

Brammer, M.J., Bullmore, E.T., et al., 1997. Generic brain activation mapping in functional magnetic resonance imaging: a nonparametric approach. Magn. Reson. Imaging 15 (7), 763–770.

Breakspear, M., Brammer, M.J., et al., 2004. Spatiotemporal wavelet resampling for functional neuroimaging data. Hum. Brain Mapp. 23 (1), 1–25.

Buchel, C., Friston, K.J., 1997. Modulation of connectivity in visual pathways by attention: cortical interactions evaluated with structural equation modelling and fMRI. Cereb. Cortex 7 (8), 768–778.

Bullmore, E.T., Suckling, J., et al., 1999. Global, voxel, and cluster tests, by theory and permutation, for a difference between two groups of structural MR images of the brain. IEEE Trans. Med. Imag 18 (1), 32–42.

Bullmore, E., Long, C., et al., 2001. Colored noise and computational inference in neurophysiological (fMRI) time series analysis: resampling methods in time and wavelet domains. Hum. Brain Mapp. 12 (2), 61–78.

Bullmore, E., Fadili, J., et al., 2003. Wavelets and statistical analysis of functional magnetic resonance images of the human brain. Stat. Methods Med. Res. 12 (5), 375–399.

Bullmore, E., Fadili, J., et al., 2004. Wavelets and functional magnetic resonance imaging of the human brain. NeuroImage 23 (Suppl. 1), S234–S249.

Chang, C., Morettin, P.A., 2005. Time domain estimation of time-varying linear systems. J. Nonparametr. Stat. 17, 365–383.

Coull, J.T., Frith, C.D., et al., 2000. Orienting attention in time: behavioural and neuroanatomical distinction between exogenous and endogenous shifts. Neuropsychologia 38 (6), 808–819.

Cui, S.Z., Li, E.Z., et al., 2000. Both sides of human cerebellum involved in preparation and execution of sequential movements. NeuroReport 11 (17), 3849–3853.

Cunnington, R., Windischberger, C., et al., 2002. The preparation and execution of self-initiated and externally-triggered movement: a study of event-related fMRI. NeuroImage 15 (2), 373–385.

Dahlhaus, R., Neumann, M.H., et al., 1999. Nonlinear wavelet estimation of time-varying autoregressive processes. Bernoulli 5 (5), 873–906.

Daubechies, I., 1988. Ortonormal bases of compactly supported wavelets. Commun. Pure Appl. Math. 41, 909–996.

Debaere, F., Wenderoth, N., et al., 2004. Changes in brain activation during the acquisition of a new bimanual coordination task. Neuropsychologia 42 (7), 855–867.

D'Esposito, M., Ballard, D., et al., 2000. The role of prefrontal cortex in sensory memory and motor preparation: an event-related fMRI study. NeuroImage 11 (5 Pt. 1), 400–408.

Eichler, M., 2005. A graphical approach for evaluating effective connectivity in neural systems. Philos. Trans. R. Soc. Lond., Ser. B Biol. Sci. 29;360 (1457), 953–967.

Friston, K.J., 1995. Functional and effective connectivity in neuroimaging: a synthesis. Hum. Brain Mapp. 2 (2), 56–78.

Friston, K., 2002. Beyond phrenology: what can neuroimaging tell us about distributed circuitry? Annu. Rev. Neurosci. 25, 221–250.

Friston, K.J., Harrison, L., et al., 2003. Dynamic causal modelling. NeuroImage 19 (4), 1273–1302.

Geweke, J., 1982. Measuring linear dependence and feedback between multiple time series. JASA 77 (378), 304–313.

Goebel, R., Roebroeck, A., et al., 2003. Investigating directed cortical interactions in time-resolved fMRI data using vector autoregressive modeling and Granger causality mapping. Magn. Reson. Imaging 21 (10), 1251–1261.

Granger, C.W.J., 1969. Investigating causal relations by econometric models and cross-spectral methods. Econometrica 37, 424–438.

Graybill, F.A., 1976. Theory and Application of the Linear Model. A: Duxbury, North Scituate.

Hall, D.A., Haggard, M.P., et al., 2000. Modulation and task effects in auditory processing measured using fMRI. Hum. Brain Mapp. 10 (3), 107–119.

Jancke, L., Himmelbach, M., et al., 2000. The effect of switching between sequential and repetitive movements on cortical activation. NeuroImage 12 (5), 528–537.

Kermadi, I., Liu, Y., et al., 2000. Do bimanual motor actions involve the dorsal premotor (PMd), cingulate (CMA) and posterior parietal (PPC) cortices? Comparison with primary and supplementary motor cortical areas. Somatosens Mot. Res. 17 (3), 255–271.

Kurata, K., Tsuji, T., et al., 2000. Activation of the dorsal premotor cortex and pre-supplementary motor area of humans during an auditory conditional motor task. J. Neurophysiol. 84 (3), 1667–1672.

Lee, K.M., Chang, K.H., et al., 1999. Subregions within the supplementary motor area activated at different stages of movement preparation and execution. NeuroImage 9 (1), 117–123.

Luppino, G., Matelli, M., et al., 1993. Corticocortical connections of area F3 (SMA-proper) and area F6 (pre-SMA) in the macaque monkey. J. Comp. Neurol. 338 (1), 114–140.

Lütkepohl, H., 1993. Introduction to Multiple Time Series Analysis. (2nd edition)Springer, Berlin.

Lutz, K., Specht, K., et al., 2000. Tapping movements according to regular and irregular visual timing signals investigated with fMRI. NeuroReport 11 (6), 1301–1306.

Matelli, M., Luppino, G., et al., 1991. Architecture of superior and mesial area 6 and the adjacent cingulate cortex in the macaque monkey. J. Comp. Neurol. 311 (4), 445–462.

Ogawa, S., Lee, T.-M., et al., 1990. Oxigenation-sensitive contrast in magnetic resonance image of rodent brain at high magnetic fields. J. Magn. Reson. Med. 14, 68–78.

Ohara, S., Mima, T., et al., 2001. Increased synchronization of cortical oscillatory activities between human supplementary motor and primary sensorimotor areas during voluntary movements. J. Neurosci. 21 (23), 9377–9386.

Raichle, M.E., MacLeod, A.M., et al., 2001. A default mode of brain function. Proc. Natl. Acad. Sci. U. S. A. 98 (2), 676–682.

Rizzolatti, G., Luppino, G., et al., 1996. The classic supplementary motor area is formed by two independent areas. Adv. Neurol. 70, 45–56.

Roebroeck, A., Formisano, E., et al., 2005. Mapping directed influence over the brain using Granger causality and fMRI. NeuroImage 25 (1), 230–242.

Rushworth, M.F., Walton, M.E., et al., 2004. Action sets and decisions in the medial frontal cortex. Trends Cogn. Sci. 8 (9), 410–417.

Sameshima, K., Baccala, L.A., 1999. Using partial directed coherence to describe neuronal ensemble interactions. J. Neurosci. Methods 94 (1), 93–103.

Sen, P.K., Singer, J.M., 1980. Large Sample Methods in Statistics—An Introduction with Applications. Chapman and Hall, London. (3. Serfling, RJ).

Stephan, K.M., Binkofski, F., et al., 1999. The role of ventral medial wall motor areas in bimanual co-ordination. A combined lesion and activation study. Brain 122 (Pt. 2), 351–368.

Talairach, J., Tournoux, P., 1988. Co-Planar Stereotaxic Atlas of the Human Brain: 3-Dimensional Proportional System: An Approach to Cerebral Imaging. Thieme Medical Pub.

Toni, I., Thoenissen, D., et al., 2001. Movement preparation and motor intention. NeuroImage 14 (1 Pt. 2), S110–S117.

Viallet, F., Massion, J., et al., 1992. Coordination between posture and movement in a bimanual load lifting task: putative role of a medial frontal region including the supplementary motor area. Exp. Brain Res. 88 (3), 674–684.

Wenderoth, N., Debaere, F., et al., 2004. Parieto-premotor areas mediate directional interference during bimanual movements. Cereb. Cortex 14 (10), 1153–1163.

Wenderoth, N., Debaere, F., et al., 2005a. The role of anterior cingulate cortex and precuneus in the coordination of motor behaviour. Eur. J. Neurosci. 22 (1), 235–246.

Wenderoth, N., Debaere, F., et al., 2005b. Spatial interference during bimanual coordination: differential brain networks associated with control of movement amplitude and direction. Hum. Brain Mapp. 26 (4), 286–300.